Structural, magnetic, electronic, and dilatation properties of the ordered solid solutions $Ln_{0.2}Sr_{0.8}CoO_{3-\delta}$ (Ln = Sm, Gd, Dy) with the same oxygen nonstoichiometry index δ

V.A. Dudnikov [1], Yu.S. Orlov [1,5], M.V. Bushinsky [4], L.A. Solovyov [2], S.N. Vereshchagin [2], S.Yu. Gavrilkin [3], A.Yu. Tsvetkov [3], M.V. Gorev [1,5], S.V. Novikov [6], O.S. Mantytskaya [4], S.G. Ovchinnikov [1,5]

[1]Kirensky Institute of Physics, Federal Research Center KSC SB RAS, 660036, Krasnoyarsk, Russia
[2]Institute of Chemistry and Chemical Technology, Federal Research Center KSC SB RAS, 660036 Krasnoyarsk, Russia
[3]Lebedev Physical Institute, 119991, Moscow, Russia
[4]Scientific-Practical Materials Research Centre NAS of Belarus, 220072, Minsk, Belarus
[5]Siberian Federal University, 660041, Krasnoyarsk, Russia
[6]Ioffe Institute of the Russian Academy of Sciences, 194021, St. Petersburg, Russia

Abstract

Single-phase samples of the layered perovskite-like cobalt oxides $Ln_{0.2}Sr_{0.8}CoO_{3-\delta}$ (Ln = Sm, Gd, Dy) with the same oxygen nonstoichiometry index $\delta = 0.37 \pm 0.01$ were synthesized. All samples are characterized by a tetragonal unit cell with the space group *I4/mmm*. The structural, magnetic, electric transport and dilatation properties of the obtained samples are investigated. The studied samples are characterized by two anomalies in magnetic properties, a high-temperature maximum near T_m = 350 K with magnetic field hysteresis below T_m, and a diffuse peak in the intermediate temperature range, which shifts with ionic radius decrease of the rare-earth element to higher temperatures. The high-temperature maxima of the magnetic susceptibility correlate with anomalies in thermal expansion, heat capacity and the features in the temperature dependences of the electrical resistivity, pointing to a strong relationship between the structural, magnetic and electronic degrees of freedom. The given comparative analysis of the experimental data of various substituting rare-earth elements with the same oxygen nonstoichiometry has been carried out for the first time.

Keywords: rare earth cobalt oxide solid solutions; layered perovskite-type cobalt oxides; structural, magnetic, electronic, and dilatation properties

Introduction

The unique physical properties of complex cobalt oxides with the perovskite structure $LnCoO_3$, when Ln is the lanthanide, have attracted the attention of researchers over the past decades due to the competition of various spin states of Co^{3+} ions. Filling the electron d^6- shell of the Co^{3+}ion in the octahedral environment of anions does not follow the Hund`s rule, and instead of the high-spin (HS) state with spin S = 2, the ground state is the low-spin (LS) term with S = 0. Many physical properties of complex oxides strongly depend on the balance between the value of the intra-atomic exchange interaction and the crystal field energy [1,2]. The possibility of various isovalent and heterovalent substitutions in these compounds with the general formula $Ln_xMe_{1-x}CoO_{3-\delta}$ (Me is an alkaline earth or rare earth metal (REM), δ is the oxygen nonstoichiometry index) leads to a great variety of magnetic, structural, electric transport properties and a strong correlation between them.

In addition to the substitution of rare earth ions by alkaline earth ions, there is another way to control the magnetic and electrical properties of cobaltites i.e. by changing the oxygen amount. A transition of ferromagnetic state to antiferromagnetic state was shown in [3] to occur when decreasing the oxygen content in $La_{0.5}Ba_{0.5}CoO_{3-\delta}$, with both phases being able to coexist. Both the ferromagnetic and antiferromagnetic phases are cubic, with oxygen vacancies being statistically distributed. In the $La_{0.5}Sr_{0.5}CoO_{3-\delta}$ system, a decrease in the oxygen content also promotes the ferromagnetic – antiferromagnetic transition, however, vacancies are ordered, leading to a crystal symmetry change at a significant content of oxygen vacancies [4]. In

addition, cobaltites are promising materials for various technological applications, in particular in hydrogen energy or as thermoelectric materials [5,6].

The generation conditions of substituted single-phase rare-earth cobaltites $Ln_{1-x}Sr_xCoO_{3-\delta}$ (Ln = La^{3+} – Yb^{3+}, Y) were determined by comprehensive analysis using electron, X-ray, and neutron diffraction. The type of cation and the value of oxygen nonstoichiometry were found to lead to the formation of a complex of superstructures (tetragonal, orthorhombic, monoclinic) with various properties [7-10]. For the elements with smaller radius than that of Nd^{3+}, there are some disordered perovskites at high temperatures, however, a structure with an ordered arrangement of the Sr^{2+}, Ln^{3+} cations and anionic vacancies at low temperatures is stable [7, 8, 11]. These disordered $Ln_{1-x}Sr_xCoO_{3-\delta}$ perovskites can be obtained in the form of metastable phases by quenching high temperature states [12]. Ordered/disordered perovskites have generally been studied in a large number of works [11, 13-15]. The effect of order – disorder transitions on the material properties is extensively investigated, with oxygen vacancies ordering in the anion sublattice being considered, the physical and chemical properties being analyzed at different levels of cation substitution in the A- position and different oxygen nonstoichiometry indices [16–20]. Despite the great number of published materials, there are no studies devoted to a comparative analysis of physical properties of solid solutions with the same level of REM doping and the same oxygen nonstoichiometry. This work is devoted to the study and comparative analysis of the physical properties of the $Ln_{0.2}Sr_{0.8}CoO_{3-\delta}$ compounds (Ln = Sm, Gd, Dy) with the same oxygen nonstoichiometry index $\delta = 0.37 \pm 0.01$.

Samples and experimental methods

The cation-ordered polycrystalline samples of $Ln_{0.2}Sr_{0.8}CoO_{3-\delta}$ (Ln = Sm, Gd, Dy) with a perovskite structure were prepared using conventional ceramic processing from a stoichiometric mixture of oxides Co_3O_4 (99.7%, metalsbasis), Sm_2O_3, Gd_2O_3, Dy_2O_3(all 99.99 %, REO), and $SrCO_3$(99.99%, metalsbasis). The purity of hygroscopic Ln_2O_3, in terms of water content, was checked additionally by TGA. Then, the powders were thoroughly mixed in an agate mortar using ethanol. The resulting mixture was annealed at T_s = 1473 Kin a corundum crucible for 24 h in air with multiple repetition of grinding-annealing cycles. After annealing, the mixture was ground again; tablets in the form of disks, with a diameter of 20 mm were pressed, then annealed in air at 1493 K for 8 hours and cooled together with the furnace to room temperature at 2 deg/min. To study thermal expansion and transport properties, the 5 x 13 x 1 ÷ 2 mm bars were cut from the samples obtained. To stabilize the oxygen content and its homogeneous distribution by volume, the samples were kept at 773 K in air for 12 hours.

Powder X-ray diffraction (PXRD) data were collected on a PANalytical X'Pert PRO diffractometer equipped with a solid state detector PIXcel using CoK_α radiation over the 2θ range 10–130°. An Anton Paar HTK 1200N camera with the automated sample alignment was used for high-temperature measurements. Powder samples were prepared by grinding with octane in an agate mortar and packed into a flat sample holder for the PXRD measurements in the Bragg-Brentano geometry. The full-profile PXRD refinement was done using the derivative difference minimization (DDM) method [21].

The oxygen content was determined with the TG-DSC NETZSCH STA 449C analyzer by the mass loss value (Δm,%) [22] when the samples are reduced in the flow of the 5% H_2-Ar mixture upon heating up to 1173 K at a rate of 10 degrees per minute, assuming that cobalt is reduced to a metallic state. The reduction occurred in a corundum crucible with a perforated lid; the mass of the samples under study was 20±0.5 mg. The measurements were performed taking into account the correction for buoyancy force, that is, the control measurements for an empty crucible (zero line) were obtained under the same conditions. The error in determining the oxygen nonstoichiometry index δ was ± 0.01.

Thermal expansion was studied in the temperature range 100–700 K in a NetzschDIL-402C induction dilatometer in dynamic mode with heating and cooling rates of 3 K/min with dry helium purge (O_2 content ≈ 0.05% of the volume). The rod load on the sample is 30 cN. The

silica glass standards were applied to calibrate the measuring system, accounting for the expansion.

The temperature and field dependences of the magnetization were measured in the temperature range from 2 to 400 K and in the fields up to 9 T using the flexible Physical Properties Measurement System (PPMS-9) Quantum Design (USA) unit, equipped with special modules for such measurements, in the center for collective use of Lebedev Physical Institute RAS (Moscow). The temperature dependences of electrical resistivity in the region of 100–700 K were obtained with the experimental set-up for thermopower and resistivity measurements [23].

Experimental

Crystal structure

PXRD analysis suggests that crystalline phase is monophasic. Annealing at a temperature of 773 K to stabilize the oxygen content and its homogeneous distribution by the sample volume resulted in the $Ln_{0.2}Sr_{0.8}CoO_{3-\delta}$ solid solutions (Ln = Sm, Gd, Dy) had the same oxygen nonstoichiometry index $\delta = 0.37 \pm 0.01$ and corresponded to the $Ln_{0.2}Sr_{0.8}CoO_{2.63}$ formula. According to X-ray diffraction analysis, the $Ln_{0.2}Sr_{0.8}CoO_{2.63}$ samples structure is a tetragonal *I*4/*mmm* superstructure (Fig. 1) with a layered ordered arrangement of A- cations, similar to that described in [24].

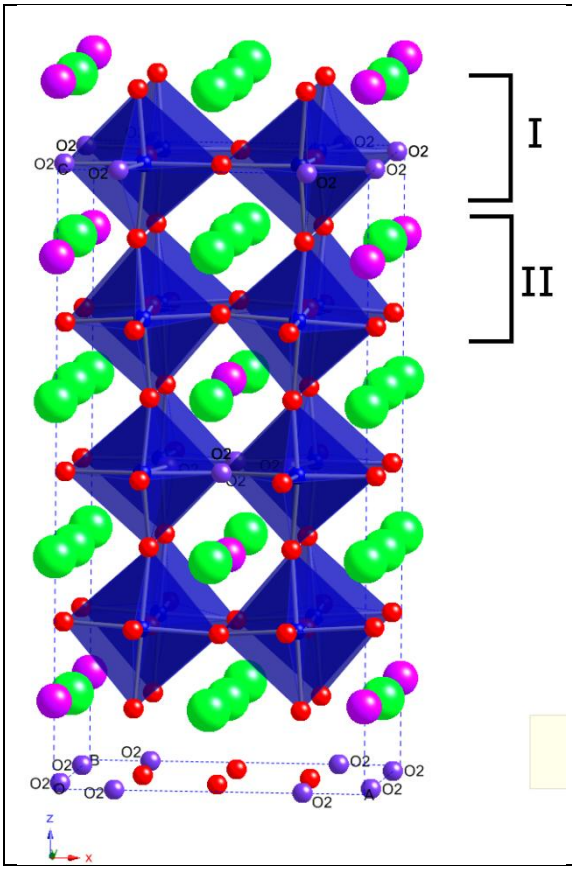

Fig. 1. The tetragonal structure of $Ln_{0.2}Sr_{0.8}CoO_{2.63}$. The octahedra correspond to Co^{3+} cations, the red and violet spheres correspond to the position of the O^{2-}/ anion vacancies, the green ones correspond to the Sr^{2+} positions, the purple spheres correspond to the positions of Ln^{3+} cations, and the O2 marks indicate the locations of oxygen vacancies.
I - $CoO_{4+\delta}$ layers in which oxygen atoms are randomly removed from O2 positions,
II - CoO_6 layers.

We gave the X-ray diffraction patterns of the samples $Gd_{0.2}Sr_{0.8}CoO_{2.63}$ and $Dy_{0.2}Sr_{0.8}CoO_{2.63}$ in [11] and [20], respectively. In the current work we have presented X-ray diffraction patterns of the $Sm_{0.2}Sr_{0.8}CoO_{2.63}$compound ordered by crystallographic A- positions (Fig. 2).

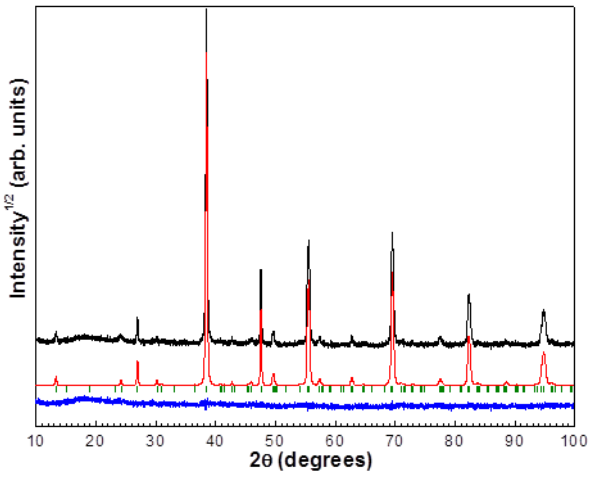

Fig. 2. Observed (top, black), calculated (mid, red), and difference (bottom, blue) PXRD profiles after DDM refinement of $Sm_{0.2}Sr_{0.8}CoO_{2.63}$ crystal structure at 298 K. The calculated peak positions are marked by ticks.

The crystal lattice parameters at T = 298 K for various Ln are given in Table 1.

Table 1. Lattice parameters of $Ln_{0.2}Sr_{0.8}CoO_{2.63}$ (Ln = Sm, Gd, Dy) samples

$Ln_{0.2}Sr_{0.8}CoO_{2.63}$	Sm	Gd	Dy
a, b (Å)	7.6847(4)	7.6844(3)	7.6802(4)
c (Å)	15.427(1)	15.402(1)	15.378(2)
V (Å^3)	911.0(1)	909.5(1)	907.1(2)

Cation arrangement in the ordered tetragonal phase based on the results of X-ray diffraction analysis is demonstrated in Fig. 1. The studied $Ln_{0.2}Sr_{0.8}CoO_{2.63}$ perovskites (Ln = Sm, Gd, Dy) structure is similar to the structure of double strontium cobaltites with rare-earth metals [24], where the A- cations are partially ordered in "columns" [25]. There are three nonequivalent positions of the A- cation in this structure, two of them are occupied by the Sr^{2+} ions; the third position is filled with randomly selected Sr^{2+} or Ln^{3+} cations (Fig. 3). The structure contains four nonequivalent oxygen positions (Fig. 1, positions O1-O4), anionic vacancies in the samples are exclusively localized in position O2 at T = 298 K (Fig. 1), which is in agreement with the data [24].

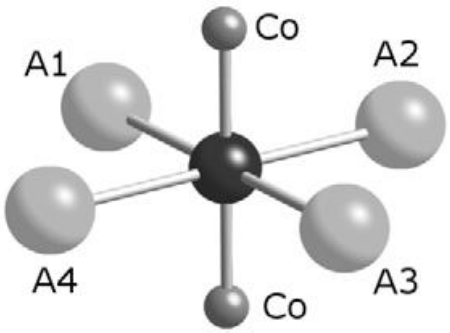

Fig. 3. The local environment of the oxygen anion O^{2-} (black sphere) in the structure of tetragonal perovskite (A1-A4 - Sr^{2+}/Ln^{3+}cations).

In the structure under consideration, the O^{2-} anions are surrounded by six cations, generally forming a distorted octahedral environment: two Co^{3+}cations at the poles and four A1-A4 cations (Sr^{2+}/Ln^{3+}) in the equatorial plane (Fig. 3). Moreover, the environment (A1-A4) of the four nonequivalent oxygen positions primarily depends on the position of the O^{2-} anion itself in crystal structure and is only partially determined by the random choice of Sr or rare-earth element.

It should be noted that X-ray diffraction analysis in the low-angle region did not show the presence of the broadened superstructure reflection observed in the $Sr_{0.9}Y_{0.1}CoO_{3-\gamma}$ compounds [10] and the associated existence of a monoclinically distorted phase described in terms of the superstructure inherent in the *A2/m* space group. We also did not observe the orthorhombic superstructure ($Cmma; 2\sqrt{2}a_p \times 4a_p \times 2\sqrt{2a_p}$) given in [26] for the $Dy_{0.2}Sr_{0.8}CoO_{2.71}$ composition, which is most likely to be associated with different oxygen nonstoichiometry of the samples.

Magnetic properties

Temperature dependences of the static magnetic susceptibility for the $Ln_{0.2}Sr_{0.8}CoO_{2.63}$ (Ln = Sm, Gd, Dy) samples obtained in zero-field cooling (ZFC) and magnetic field cooling *H* = 0.5 T (FC) are shown in Fig. 4 (a) - 6 (a). Above room temperature all the studied compositions are characterized by a sharp maximum, which slightly shifts to lower temperatures with a decrease in the ionic radius of the rare-earth element (R_{Sm3+} = 1.24 Å , R_{Gd3+} = 1.215Å, R_{Dy3+} = 1.19 Å [27]). This is clearly seen in Fig. 7, presented for clarity. In the intermediate temperature range between 50 and 300 K, a peak is also observed for all $Ln_{0.2}Sr_{0.8}CoO_{2.63}$ (Ln = Sm, Gd, Dy), which is strongly broad in temperature, and with a decrease in the rare earth ionic radius, is characterized by a shift to higher temperatures, in contrast to the high-temperature maximum. With decreasing temperature (T < 50 K) for $Ln_{0.2}Sr_{0.8}CoO_{2.63}$ (Ln = Gd, Dy), a sharp increase in magnetization is observed, associated with a large paramagnetic moment of Gd^{3+} and Dy^{3+} ions (for free Gd^{3+} and Dy^{3+} ions, the effective magnetic moments are $\mu_{theor}(\mu_B)$ = 7.94 and 10.6, respectively [28]). For $Sm_{0.2}Sr_{0.8}CoO_{2.63}$ in both ZFC and FC measurement modes, an increase in the susceptibility at low temperatures was not noted (Fig. 4a), which is probably due to the small effective magnetic moment of the Sm^{3+} ions (μ_{theor} = 1.55 μ_B), although for $LnCoO_3$ (Ln = Sm, Gd, Dy) compounds [29, 30], the increase in the susceptibility at low temperatures is characteristic of all compositions.

In the helium temperature range for $Sm_{0.2}Sr_{0.8}CoO_{2.63}$, a magnetic transition is observed in the temperature dependence of the magnetic susceptibility (Fig. 4a, inset), resulting in a shift of the hysteresis loop at T = 2 K (Fig. 4b, inset). The field dependences of the magnetization are given in Fig. 4 (b) - 6 (b). The field hysteresis is most pronounced for $Sm_{0.2}Sr_{0.8}CoO_{2.63}$ in the magnetization isotherms at T = 2 K. The field hysteresis is retained up to temperatures of ~ 350÷360 K, here, the broadening of the hysteresis loop in the region of strong fields rapidly disappears with increasing temperature for $Gd_{0.2}Sr_{0.8}CoO_{2.63}$ and $Dy_{0.2}Sr_{0.8}CoO_{2.63}$.

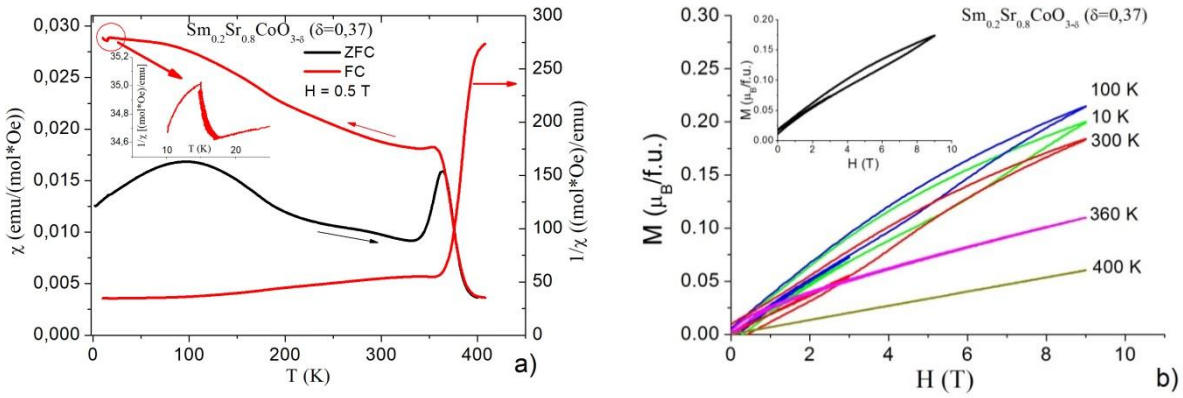

Fig. 4. Temperature dependences of the molar and inverse magnetic susceptibilities (a) and magnetization isotherms (b) of the $Sm_{0.2}Sr_{0.8}CoO_{2.63}$ compound. In the inset to Fig. (a) the behavior of the inverse magnetic susceptibility in the magnetic transition region is shown, in the inset to Fig. (b) the field dependence of the magnetization at T = 2 K is given.

In the region of 300 K, the coercive force (H_{coer}) and remanent magnetization (M_{res}) maxima are observed for all samples, taking the values H_{coer} = 4.52 kOe, 2.15 kOe, 3.95 kOe and M_{res} = 0.0095, 0.0074, 0.028 μ_B/f.u for the Sm, Gd and Dy compounds, respectively. A further temperature increase leads to the H_{coer} and M_{res} decrease, and the type of the magnetization isotherms corresponds to paramagnetic behavior at T = 400 K.

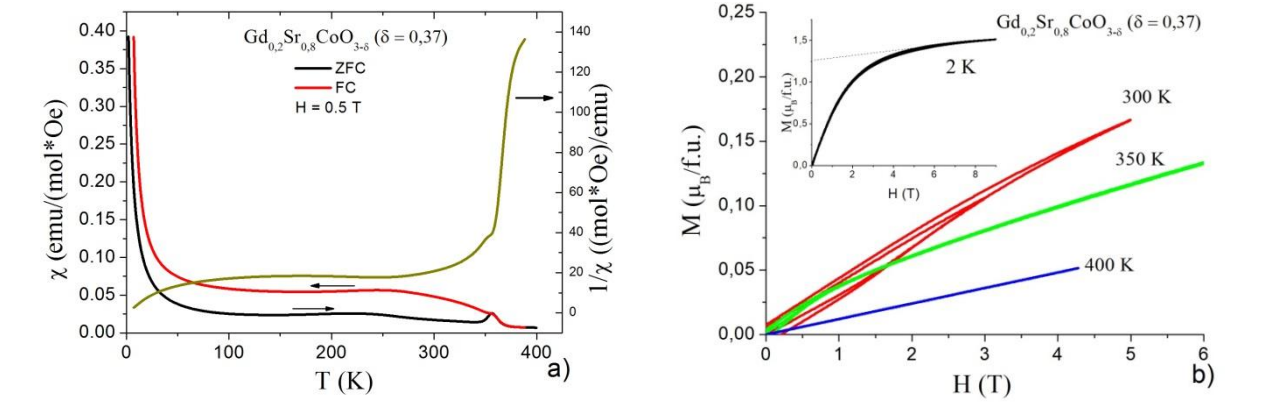

Fig. 5. Temperature dependences of the molar and inverse magnetic susceptibilities (a) and magnetization isotherms (b) of the $Gd_{0.2}Sr_{0.8}CoO_{2.63}$ compound. The field dependence of the magnetization at T = 2 K is depictedin the inset to Fig. (b).

An accurate determination of the saturation magnetization (M_{sut}) is not possible due to the absence of saturation in fields up to 10 T. A rough estimate gives M_{sut} = 0.05, 1.25 and 1.1 μ_B/f.u for Sm, Gd и Dy compounds, respectively (Fig. 4-6 (b), inserts). These values are significantly lower than the expected contributions from non-interacting rare earth elements (0.2 x $\mu_{eff}(Re^{3+})$), being equal to 0.17, 1.56, and 2.13μ_B for Sm^{3+}, Gd^{3+} и Dy^{3+} respectively. The given difference suggests a magnetic interaction between the sublattices of the rare-earth element and cobalt, similar to the observed magnetic coupling in the $Ho_{0.5}Nd_{0.5}Fe_3(BO_3)_4$ compounds between the Nd^{3+}, Ho^{3+} and Fe^{3+} ions [31].

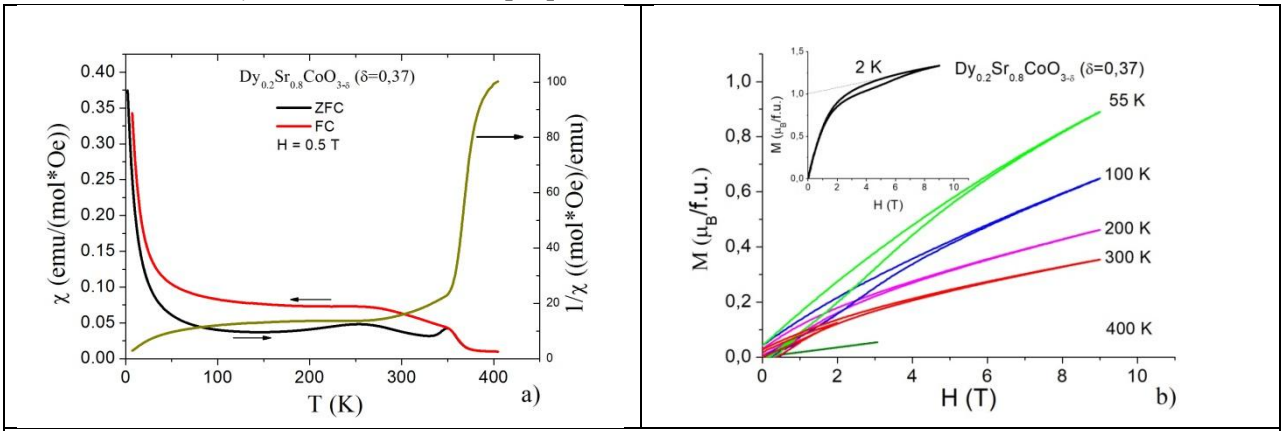

Fig. 6. Temperature dependences of the molar and inverse magnetic susceptibilities (a) and the magnetization isotherms (b) of the $Dy_{0.2}Sr_{0.8}CoO_{2.63}$ compound. The field dependence of the magnetization at T = 2 K is illustrated in the inset to Fig. (b).

Temperature dependences of the inverse magnetic susceptibility of the samples under study are shown in Fig. 4 (a) - 6 (a). The dependences are not approximated by straight lines in the studied temperature range (up to 360 K). Thus, the $\chi(T)$ dependences do not obey Curie ($\chi \sim C/T$) or Curie-Weiss ($\chi \sim C/(T-\Theta)$) laws. The high temperature range about 400 K, with paramagnetic behavior according to the field dependences of the magnetization observed, is too small to reliably determine the asymptotic Curie temperatures followed by the calculation of effective magnetic moments.

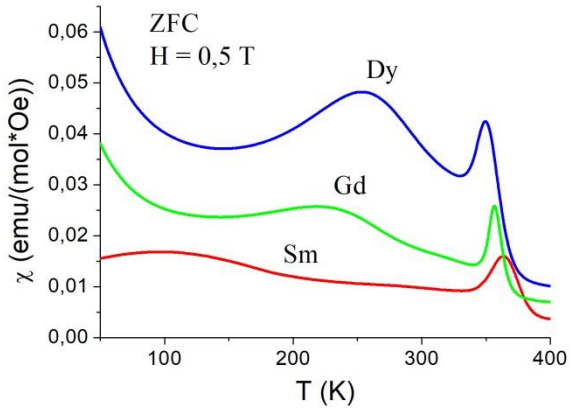

Fig. 7. Temperature dependences of molar magnetic susceptibility in the temperature range from 50 to 400 K, obtained in the ZFC mode for the $Ln_{0.2}Sr_{0.8}CoO_{2.67}$ (Ln = Sm, Gd, Dy) samples.

Thermal expansion

Temperature dependences of the thermal volume expansion coefficient β of the $Ln_{0.2}Sr_{0.8}CoO_{2.67}$ (Ln = Sm, Gd, Dy) samples is illustrated in Fig. 8 (a). A sharp minimum is observed on the β(T) curves for all the studied compositions, which is also reflected by the anomalous behavior of the strain ΔL/L in the temperature range 300–450 K, (Fig. 8 b). The anomaly in the heat capacity noted for the $Gd_{0.2}Sr_{0.8}CoO_{2.63}$ compound [11] in the same temperature range correlates with the minimum in temperature dependences of the thermal expansion coefficient. These sharp minima correspond well to the high temperature peaks for magnetic susceptibility in Fig. 7.

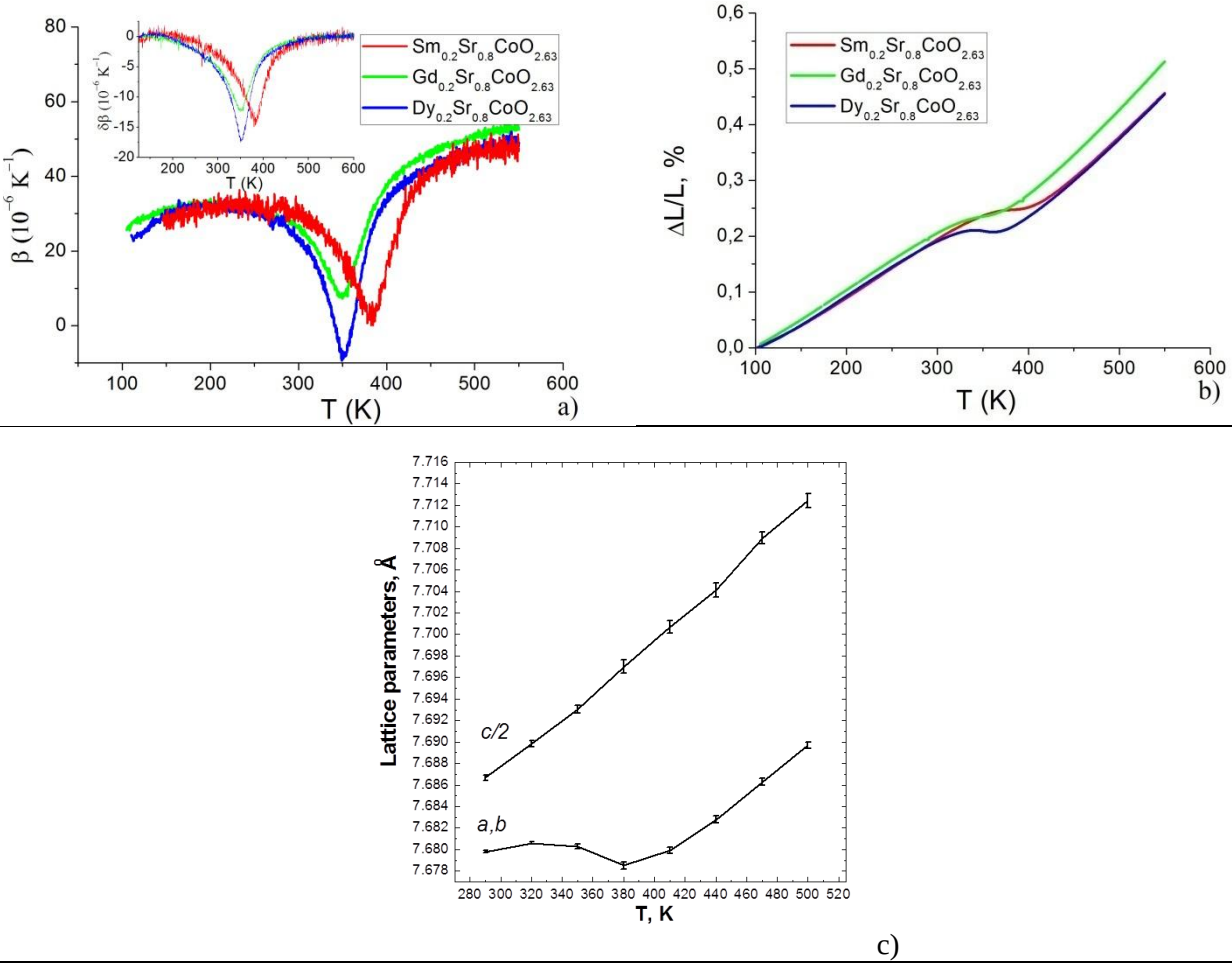

Fig. 8. Temperature dependences of the coefficient of volumetric thermal expansion β (Fig. (a)),

strain ΔL/L (Fig. (b)) and lattice parameters (c) in the temperature range from 285 to 500 K. The anomalous contribution to thermal expansion is shown in the inset in Fig. (a).

X-ray diffraction studies of the $Dy_{0.2}Sr_{0.8}CoO_{2.63}$ sample in the temperature range 285–500 K (Fig. 8 c) revealed the anomalous lattice contraction in the (a, b) plane and the absence of anomalies along the *c*axis. Nevertheless the space group of symmetry does not change. A slight discrepancy in the temperature minima can be explained by the fact that the temperature dependences of the coefficient of volumetric thermal expansion β(T) were obtained on bulk samples, while the crystal lattice parameters were derived from the X-ray diffraction.

Electrical resistance

The electrical resistance was measured in the range from 100 to 700 K. Temperature dependences of the electrical resistivity ρ (T) are presented in Fig. 9 and qualitatively correspond to the semiconductor type $d\rho(T)/d(T) < 0$ up to temperatures when observed a high-temperature magnetic transition. In this case, the behavior of electrical resistance in the low-temperature region is best described in terms of the Mott`s three-dimensional conductivity model (Fig. 9, inset). As the temperature subsequently rises (in the magnetic transition field), a bending in the ρ (T) dependences obviously associated with additional scattering of charge carriers on magnetic fluctuations in the magnetic transition field is observed.

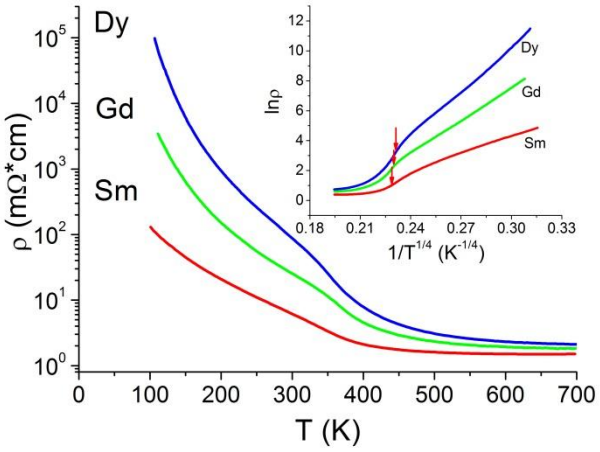

Fig. 9. Temperature dependences of the electrical resistivity of the $Ln_{0.2}Sr_{0.8}CoO_{2.67}$ (Ln = Sm, Gd, Dy) samples within the temperature range from 100 to 700 K. In the inset the Mott law in the log scale is shown. The red arrows indicate the high temperature magnetic peculiarities peaks from Fig. 7.

Discussion

We have found the clear correlation of the temperature dependences of magnetic susceptibility, lattice expansion and electrical resistivity. The high temperature narrow peaks of magnetic susceptibility at T = 350-370 K in Fig. 7 shift with the Ln ionic radius in the same way as the minima in the thermal expansion coefficient in Fig. 8 and in the same way as electrical resistivity peculiarities shown in Fig. 9. To understand the origin of these peaks we compare our results with the literature. The first question concerns the charge state of the Co ion. In many other metal oxides with dominant ionic bonding like manganites the substitution of the Ln^{3+} ion by Sr^{2+} ion results in the change of the *3d* ion valence, one may expect Co^{4+} appearance to restore the electroneutrality. Nevertheless due to oxygen vacancies the concentration of Co^{4+} for our composition is not large and equal to 6%. Our previous XANES measurements at the Co *K*-edge of the single crystalline $Gd_{0.4}Sr_{0.6}CoO_{2.85}$ did not found any change of the Co ion valence [32].

Thus in our discussion below we consider only Co^{3+} ions that may be in different crystallographic positions and in different spin states. The rare-earth cobalt oxides with ordered oxygen vacancies and partial substitution of Ln element by divalent metals like Sr or Ba have been actively discussed recently, especially their magnetic properties [33-39]. In the most

relevant paper [39] with the high resolution XRD and neutron diffraction the sample composition $Sr_3YCo_4O_{10.72}$ that is equivalent to $Sr_{0.75}Y_{0.25}CoO_{2.68}$ is rather close to our composition with the Sm, Gd and Dy ions instead of Y. According to [39] in the tetragonal phase *I*4/*mmm* there are nonequivalent Co positions in CoO_6 octahedra and in CoO_4 tetrahedra shown in Fig. 1 above. The ferrimagnetic phase in $Sr_3YCo_4O_{10.72}$ appears below T_m = 360K and the paramagnetic-ferrimagnetic transition does not coincide with several structural transitions found in [39]. Ferrimagnetism occurs within two almost antiferromagnetic sublattices with slightly different magnetic moments of sublattices. The Co^{3+} ions in tetrahedral positions have large magnetic moment 4 μ_B [39] that is associated with the HS state, the Co^{3+} ions in the octahedral positions have small moment $1.16\mu_B$. Obviously these ions are mixtures of the HS and LS with dominant contribution of the LS state. Indeed, rather small external pressure 2 GPa can stabilize the LS state [40]. Due to the known lanthanoid compression decreasing ionic radii results in the increasing the crystal field and stabilization the LS state for heavy Ln elements. Starting from La and for all Ln the LS spin state is stable in the octahedral coordination, as is well known for all $LnCoO_3$ compounds. The value of spin gap, the energy E_{HS}-E_{LS} has been estimated in [41]. Below 550K the crystal structure of $Sr_3YCo_4O_{10.72}$ has the symmetry *Cmma* with additional superstructure and third nonequivalent Co^{3+} ion position with magnetic moment 2.7 μ_B [39]. Our samples with another Ln ion did not reveal this phase, so we will restrict ourselves to HS tetrahedral and LS octahedral Co^{3+} ions.

The sharp peaks in Fig. 7 at 350 K for Dy, 356 K for Gd and 364 K for Sm we relate with the ferrimagnetic transition temperature T_m, that is close to T_m = 360 K in [39]. The magnetic hysteresis below T_m shown if Figs 4-6 confirms the ferromagnetic magnetic order. While the XRD in $Sr_3YCo_4O_{10.72}$ did not reveal structural changes at T_m [39], our thermal expansion measurements for Dy, Gd and Sm cobaltites demonstrate some anomalies in thermal volume expansion coefficient β and lattice parameters related to T_m. These anomalies are some isostructural deformations, and the sharp minima in Fig. 8 corresponds the variation of T_m for Dy, Gd and Sm. The same temperatures are related to the changes in the temperature dependence of resistivity in Fig. 9. The correlation of the conductivity with magnetic phase transition is a common phenomenon in narrow band materials [42].

As concerns the low temperature wide and smooth maxima in magnetic susceptibility in Fig. 7 we related it with the temperature occupation of the HS octahedral Co^{3+} ions. The largest spin gap for Dy and the smallest spin gap for Sm reveal itself with different temperatures of the maxima. Substitution of Ln^{3+}ions by divalent Sr^{2+} ions with a large ionic radius (R_{Sr}^{2+} = 1.44 Å, z = 12) [27] enhances the oxygen octahedra distortions and the unit cell volume [43]. Nevertheless, taking into account the disorder in the arrangement of Ln^{3+} and Sr^{2+} ions in terms of A- positions of the crystal lattice, this leads to the fact that, some of the Co^{3+} ions in the octahedral environment in the substituted $Ln_{1-x}Sr_xCoO_{3-\delta}$ cobaltites can be found in the HS state even at low temperatures [44]. With increasing temperature, the rest of Co^{3+} ions in the LS- state goes into the HS- state, as evidenced by the maximum in the intermediate temperature range on the temperature dependences of the magnetic susceptibility (Fig. 7), which explicitly shifts to higher temperatures as the ion radius of the rare-earth ion decreases. Finally, the low temperature upturn of the susceptibilities in Figs. 4-7 is obviously related with the f-electron contribution.

Conclusion

The synthesized single-phase samples of layered perovskite-like rare-earth cobalt oxides $Ln_{0.2}Sr_{0.8}CoO_{3-\delta}$ (Ln = Sm, Gd, Dy) with the same oxygen nonstoichiometry index δ = 0.37± 0.01 have been characterized by a tetragonal unit cell with the space group *I4/mmm*. The study of structural, magnetic, electric transport and dilatation properties of the samples has allowed one to carry out the comparative analysis. The obtained samples are characterized by two anomalies in magnetic properties i.e. the high-temperature maximum near T = 350 K, and the diffuse peak in the intermediate temperature range, which shifts with ionic radius decrease of the rare-earth

element to higher temperatures. The high-temperature maxima in the temperature dependences of the magnetic susceptibility correlate with anomalies in thermal expansion, heat capacity and the features in the temperature dependences of the electrical resistivity. A magnetic transition for the $Sm_{0.2}Sr_{0.8}CoO_{2.63}$ compound at helium temperatures was found.

Acknowledgments

The work was financially supported by Russian Foundation for Basic Research (grant No. 19-03-00017); RFBR and BRFFR as a part of scientific project No. 18-52-00017 and project F18R-119; Russian Foundation for Basic Research, Government of Krasnoyarsk Territory, Krasnoyarsk Regional Fund of Science to the research project: «New thermoelectric materials based on multi-scale spatially inhomogeneous substituted rare-earth cobalt oxides and the Ruddlesden-Popper phases» project No. 18-42-243004, Project of Basic Research SB RAS V.45.3.3.

References:

[1] M. Imada, A. Fujimori, Y. Tokura, Metal-insulator transitions, Reviews of modern physics 70 (1998) 1039. https://doi.org/10.1103/RevModPhys.70.1039.

[2] J.B. Goodenough, Electronic and ionic transport properties and other physical aspects of perovskites, Reports on Progress in Physics 67 (2004) 1915. https://doi.org/10.1088/0034-4885/67/11/R01.

[3] I.O. Troyanchuk, D.V. Karpinsky, M.V. Bushinsky, V. Sikolenko, V. Efimov, A. Cervellino, Pis'mavZhETF 93 (2011) 139-143. https://doi.org/10.1134/S0021364011030167.

[4] I.O. Troyanchuk, D.V. Karpinsky, M.V. Bushinsky, A.V. Nikitin, V.M. Dobryansky, Ferromagnet – antiferromagnet transition in the $La_{0.5}Sr_{0.5}CoO_{3-\delta}$ cobaltite system, Bulletin of BSU 1(3) (2012), 56-59. http://elib.bsu.by/handle/123456789/49217.

[5] Natal'ya B. Ivanova, Sergei G. Ovchinnikov, Maksim M. Korshunov, Il'ya M. Eremin and Natal'ya V. Kazak, Specific features of spin, charge, and orbital ordering in cobaltites, Physics-Uspekhi 52 (2009) 789. https://doi.org/10.3367/UFNe.0179.200908b.0837

[6] V.A. Dudnikov, Yu.S. Orlov, N.V. Kazak, M.S. Platunov, S.G. Ovchinnikov, Anomalies of the electronic structure and physical properties of rare-earth cobaltites near spin crossover, JETP Letters 104 (2016) 588-600. https://doi.org/10.1134/S002136401620011X.

[7] Michael James, Liliana Morales, Kia Wallwork, Maxim Avdeev, Ray Withers, Darren Goossens, Structure and magnetism in rare earth strontium-doped cobaltates, Physica B: Condensed Matter 385-386 (2006) 199-201. https://doi.org/10.1016/j.physb.2006.05.244.

[8] M. James, T. Tedesco, D.J. Cassidy, R.L. Withers, Oxygen vacancy ordering in strontium doped rare earth cobaltate perovskites $Ln_{1-x}Sr_xCoO_{3-\delta}$ (Ln= La, Pr and Nd; x> 0.60), Materials research bulletin 40 (2005) 990-1000. https://doi.org/10.1016/j.materresbull.2005.02.020.

[9] I.O. Troyanchuk, D.V. Karpinsky, M.V. Bushinsky, V. Sikolenko, V. Efimov, A. Cervellino, and B. Raveau, The ferromagnetic and antiferromagnetic phases in anion deficient $La_{0.5-x}Pr_xBa_{0.5}CoO_{3-\delta}$ cobaltites, Journal of Applied Physics 112 (2012) 013916. https://doi.org/10.1063/1.4733953.

[10] I.O. Troyanchuk, M. V. Bushinsky R. A. Lanovsky V. V. Sikolenko C. Ritter, Magnetic Properties of a Layered Cobaltite $Sr_{1-x}Y_xCoO_{3-\delta}$ (x = 0.1), Physics of the Solid State 60 (2018) 1999-2005. https://doi.org/10.1134/S1063783418100281.

[11] V.A. Dudnikov, Yu. S. Orlov, S. Yu. Gavrilkin, M.V. Gorev, S.N. Vereshchagin, L.A. Solovyov, N.S. Perov, S.G. Ovchinnikov, Effect of Gd and Sr ordering in A sites of doped $Gd_{0.2}Sr_{0.8}CoO_{3-\delta}$ perovskite on its structural, magnetic, and thermodynamic properties, The Journal of Physical Chemistry C 120 (2016) 13443-13449. https://doi.org/10.1021/acs.jpcc.6b04810.

[12] Sergei N. Vereshchagin, Leonid A. Solovyov, Evgenii V. Rabchevskii, Vyacheslav A. Dudnikov, Sergey G. Ovchinnikovb and Alexander G. Anshits, Methane oxidation over A- site ordered and disordered $Sr_{0.8}Gd_{0.2}CoO_{3-\delta}$ perovskites, Chemical Communications 50 (2014) 6112-6115. https://doi.org/10.1039/C4CC00913D.

[13] S.Ya Istomin, O.A. Drozhzhin, G. Svenssonc, E.V. Antipov, Synthesis and characterization of $Sr_{1-x}Ln_xCoO_{3-\delta}$, Ln = Y, Sm–Tm, $0.1 \leq x \leq 0.5$, Solid state sciences 6 (2004) 539-546. https://doi.org/10.1016/j.solidstatesciences.2004.03.029.

[14] R.L. Withers, M. James, and D.J. Goossens, Atomic ordering in the doped rare earth cobaltates $Ln_{0.33}Sr_{0.67}CoO_{3-\delta}$ (Ln = Y^{3+}, Ho^{3+} and Dy^{3+}), Journal of Solid State Chemistry174 (2003) 198-208. https://doi.org/10.1016/S0022-4596(03)00227-5.

[15] B. Raveau, V. Pralong, V. Caignaert, M. Hervieu and A. Maignan, Primordial role of cobalt valence in the magnetotransport properties of oxygen deficient perovskites $Sr_{1-x}Ln_xCoO_{3-\delta}$, Journal of Physics: Condensed Matter 17 (2005) 7371. https://doi.org/10.1088/0953-8984/17/46/021.

[16] S.Ya Istomin, J. Grins, G. Svensson, O.A. Drozhzhin, V.L. Kozhevnikov, E.V. Antipov, J.P. Attfield, Crystal structure of the novel complex cobalt oxide $Sr_{0.7}Y_{0.3}CoO_{2.62}$, Chemistry of materials 15 (2003) 4012-4020. https://doi.org/10.1021/cm034263e.

[17] A. Maignan, S. Hébert, V. Caignaert, V. Pralong, D. Pelloquin, $Sr_{2/3}Y_{1/3}CoO_{8/3+\delta}$: Transition from insulating antiferromagnet to metallic ferromagnet by control of the oxygen content, Journal of Solid State Chemistry, 178 (2005) 868-873. https://doi.org/10.1016/j.jssc.2004.12.014.

[18] Shun Fukushima, Tomonori Sato, Daisuke Akahoshi, and Hideki Kuwahara, Order–Disorder Effect of A-site and Oxygen-Vacancy on Magnetic and Transport Properties of $Y_{1/4}Sr_{3/4}CoO_{3-\delta}$, Journal of the Physical Society of Japan 78 (2009) 064706. https://doi.org/10.1143/JPSJ.78.064706.

[19] Li Feng, and Jun Fang, Glassy-ferromagnetic behavior in $Eu_{0.5}Sr_{0.5}CoO_3$, Journal of Magnetism and Magnetic Materials 324 (2012) 2664-2668. https://doi.org/10.1016/j.jmmm.2012.03.046.

[20] V.A. Dudnikov, Yu.S. Orlov, N.V. Kazak, A.S. Fedorov, L.A. Solov'yov, S.N. Vereshchagin, A.T. Burkov, S.V. Novikov, S.G.Ovchinnikov, Thermoelectric properties and stability of the $Re_{0.2}Sr_{0.8}CoO_{3-\delta}$ Re = Gd, Dy) complex cobalt oxides in the temperature range of 300–800 K, Ceramics International 45 (2019) 5553-5558. https://doi.org/10.1016/j.ceramint.2018.12.013.

[21] Leonid A. Solovyov, Full-profile refinement by derivative difference minimization, Journal of Applied Crystallography 37 (2004) 743-749. https://doi.org/10.1107/S0021889805004899.

[22] K. Conder, E. Pomjakushina, A. Soldatov, & E. Mitberg, Oxygen content determination in perovskite-type cobaltates, Materials research bulletin 40 (2005) 257-263. https://doi.org/10.1016/j.materresbull.2004.10.009.

[23] A.T. Burkov, A. Heinrich, P.P. Konstantinov, T. Nakama, & K. Yagasaki, Experimental set-up for thermopower and resistivity measurements at 100-1300 K, Measurement Science and Technology 12 (2001) 264. https://doi.org/10.1088/0957-0233/12/3/304.

[24] M. James, D. Cassidy, D.J. Goossens and R.L. Withers, The phase diagram and tetragonal superstructures of the rare earth cobaltate phases $Ln_{1-x}Sr_xCoO_{3-\delta}$ (Ln = La^{3+}, Pr^{3+}, Nd^{3+}, Sm^{3+}, Gd^{3+}, Y^{3+}, Ho^{3+}, Dy^{3+}, Er^{3+}, Tm^{3+} and Yb^{3+}), J. Solid State Chem 177 (2004) 1886-1895. https://doi.org/10.1016/j.jssc.2004.01.012.

[25] G. King, P.M. Woodward, Cation ordering in perovskites, J. Mater. Chem. 20 (2010) 5785-5796. https://doi.org/10.1039/b926757c.

[26] M. James, M. Avdeev, P. Barnes, L. Morales, K. Wallwork, R. Withers, Orthorhombic superstructures within the rare earth strontium-doped cobaltate perovskites: $Ln_{1-x}Sr_xCoO_{3-\delta}$ (Ln = Y^{3+}, Dy^{3+}–Yb^{3+}; 0.750 < x < 0.875), Journal of Solid State Chemistry 180 (2007) 2233-2247. https://doi.org/10.1016/j.jssc.2007.04.029.

[27] Robert D. Shannon, Revised effective ionic radii and systematic studies of interatomic distances in halides and chalcogenides, Acta crystallographica section A: crystal physics, diffraction, theoretical and general crystallography 32 (1976) 751-767. https://doi.org/10.1107/s0567739476001551.

[28] C. Kittel, Introduction to solid state physics, NewYork: Wiley, 1976.

[29] J. Gutiérrez Seijas, J. Prado-Gonjal, D.A. Brande, I. Terry, E. Moran and R. Schmidt, Microwave-Assisted Synthesis, Microstructure, and Magnetic Properties of Rare-Earth Cobaltites, Inorg. Chem. 56 (2017) 627−633. https://doi.org/10.1021/acs.inorgchem.6b02557.

[30] Yu.S. Orlov, L.A. Solovyov, V.A. Dudnikov, A.S. Fedorov, A.A. Kuzubov, N.V. Kazak, V.N. Voronov, S.N. Vereshchagin, N.N. Shishkina, N.S. Perov, K.V. Lamonova, R.Yu. Babkin, Yu.G. Pashkevich, A.G. Anshits, S.G. Ovchinnikov, Structural properties and high-temperature spin and electronic transitions in $GdCoO_3$: Experiment and theory, Physical Review B 88 (2013) 235105. https://doi.org/10.1103/PhysRevB.88.235105.

[31] M. Platunov, N. Kazak, V. Dudnikov, V. Temerov, I. Gudim, Yu. Knyazev, S. Gavrilkin, V. Dyadkin, I. Dovgaliuk, D. Chernyshov, A. Hen, F. Wilhelm, A. Rogalev, S. Ovchinnikov, Element selective magnetism in $Ho_{0.5}Nd_{0.5}Fe_3(BO_3)_4$ single crystal probed with hard X-ray magnetic circular dichroism, Journal of Magnetism and Magnetic Materials 479 (2019) 312-316. https://doi.org/10.1016/j.jmmm.2019.02.040.

[32] M.S. Platunov, V.A. Dudnikov, Yu.S. Orlov, N.V. Kazak, L.A. Solovyov, Ya.V. Zubavichus, A.A. Veligzhanin, P.V. Dorovatovskii, S.N. Vereshchagin, K.A. Shaykhutdinov, S.G. Ovchinnikov, Crystal structure and electronic states of Co and Gd ions in a $Gd_{0.4}Sr_{0.6}CoO_{2.85}$ single crystal, JETP letters, 103, (2016) 196-200. https://doi.org/10.1134/S0021364016030139.

[33] I.O. Troyanchuk, D.V. Karpinsky, A.P. Sazonov, V. Sikolenko, V. Efimov, A. Senyshyn, Effect of iron doping on magnetic properties of $Sr_{0.78}Y_{0.22}CoO_{2.625+\delta}$ - layered perovskite, Journal of materials science 44 (2009) 5900-5908. https://doi.org/10.1007/s10853-009-3835-7.

[34] D.V. Sheptyakov, V.Yu. Pomjakushin, O.A. Drozhzhin, S.Ya. Istomin, E.V. Antipov, I.A. Bobrikov, and A.M. Balagurov, Correlation of chemical coordination and magnetic ordering in $Sr_3YCo_4O_{10.5+\delta}$ (δ = 0.02 and 0.26), Physical Review B 80 (2009) 024409. https://doi.org/10.1103/PhysRevB.80.024409.

[35] M. James, K.S. Wallwork, R.L. Withers, D.J. Goossens, K.F. Wilson, J. Horvat, X.L. Wang, M. Colella, Structure and magnetism in the oxygen-deficient perovskites $Ce_{1-x}Sr_xCoO_{3-\delta}$ ($x \geq 0.90$), Materials research bulletin 40 (2005) 1415-1431. https://doi.org/10.1016/j.materresbull.2005.03.025.

[36] D.J. Goossens, K.F. Wilson, and M. James, Structure and magnetism in $Ho_{1-x}Sr_xCoO_{3-\delta}$, Journal of Physics and Chemistry of Solids 66 (2005) 169-175. https://doi.org/10.1016/j.jpcs.2004.09.003.

[37] R. Ang, Y.P. Sun, X.B. Zhu, W.H. Song, X.G. Luo, X.H. Chen, Spin-state transition, magnetic, electrical and thermal transport properties of the perovskite cobalt oxide $Gd_{0.7}Sr_{0.3}CoO_3$, Solid state communications 138 (2006) 255-260. https://doi.org/10.1016/j.ssc.2006.02.027.

[38] D.J. Goossens, K.F. Wilson, M. James, A.J. Studer, and X.L. Wang, Structural and magnetic properties of $Y_{0.33}Sr_{0.67}CoO_{2.79}$, Physical Review B 69 (2004) 134411. https://doi.org/10.1103/PhysRevB.69.134411.

[39] D.D. Khalyavin, L.C. Chapon, E. Suard, J.E. Parker, S.P. Thompson, A.A. Yaremchenko, and V.V. Kharton, Complex room-temperature ferrimagnetism induced by zigzag stripes of oxygen vacancies in $Sr_3YCo_4O_{10+\delta}$, Physical Review B 83 (2011) 140403. https://doi.org/10.1103/PhysRevB.83.140403.

[40] N.O. Golosova, D.P. Kozlenko, L.S. Dubrovinsky, O.A. Drozhzhin, S.Ya. Istomin, and B.N. Savenko, Spin state and magnetic transformations in $Sr_{0.7}Y_{0.3}CoO_{2.62}$ at high pressures Phys. Rev. B 79 (2009) 104431. https://doi.org/10.1103/PhysRevB.79.104431.

[41] S.G. Ovchinnikov, Yu.S. Orlov, V.A. Dudnikov, Temperature and field dependent electronic structure and magnetic properties of $LaCoO_3$ and $GdCoO_3$, Journal of Magnetism and Magnetic Materials 324 (2012) 3584-3587. https://doi.org/10.1016/j.jmmm.2012.02.096.

[42] N.F. Mott, Metal-Insulator transitions, Taylor and Francis, London, 1974.

[43] V.A. Dudnikov, N.V. Kazak, Yu.S. Orlov, S.N. Vereshchagin, S.Yu. Gavrilkin, A. Yu. Tsvetkov, M.V. Gorev, A.A. Veligzhanin, A.L. Trigub, I.O. Troyanchuk, S.G. Ovchinnikov, Structural, Magnetic, and Thermodynamic Properties of Ordered and Disordered Cobaltite $Gd_{0.1}Sr_{0.9}CoO_{3-\delta}$, Journal of Experimental and Theoretical Physics 128 (2019), 630-640. https://doi.org/10.1134/S1063776119020171.

[44] T.N. Vasil'chikova, T.G. Kuz'mova, A.A. Kamenev, A.R. Kaul', A.N. Vasil'ev, Spin states of cobalt and the thermodynamics of $Sm_{1-x}Ca_xCoO_{3-\delta}$ solid solutions, JETP letters 97 (2013) 34-37. https://doi.org/10.1134/S002136401301013X.